Bulletin of the Seismological Society of America, Vol. 99, No. 2B, pp. 1091–1102, May 2009, doi: 10.1785/0120080288

Single-Couple Component of Far-Field Radiation from Dynamical Fractures

by Leon Knopoff and Yun-Tai Chen

Abstract We reexamine two canons of the seismological literature, that elastic displacements in the far field are proportional to slip velocities on the dynamical fault surface, and that dynamical in-plane slip on an earthquake fault has a double-couple body force equivalent. We show that if faulting takes place on a fault of finite thickness, and there is a strength-weakening zone near the advancing crack tip, there is an additional single-couple term in the body force equivalence and additional terms in the far-field displacement, which are proportional to the time rate of increase of stress drop in the advancing weakening zone. We also show that the single-couple equivalent does not violate principles of Newtonian mechanics because the torque imbalance in the single couple is counterbalanced by rotations within the fault zone; the crack therefore radiates torque waves and a rotational deformation field.

Introduction

The proportionality between elastic displacements in the far field and slip velocities on a dynamical fault surface (Knopoff and Gilbert, 1960; Haskell, 1964, 1966) and the statement that dynamical in-plane slip on an earthquake fault has a double-couple body force equivalent (Knopoff and Gilbert, 1960; Maruyama, 1963; Burridge and Knopoff, 1964; Stauder and Bollinger, 1964, 1966) are two canons of the seismological literature. The first is a basis for calculations of seismic energy radiated from earthquake events (Knopoff and Gilbert, 1960; Haskell, 1964, 1966; Kostrov, 1970, 1974), and the second is a basis for seismic moment calculations (Aki, 1966). These two statements are directly related. We show that both statements must be modified if a fracture takes place on a fault of finite thickness and if there is a strength-weakening zone near the advancing crack tip.

The statement of proportionality between the far-field displacement and the slip velocity would appear to be contradicted by classical integrations of the scalar wave equation by Kirchhoff in 1882 (Born and Wolf, 1959, pp. 374–377) and the elastic wave equation by Knopoff (1956) and Knopoff and Gilbert (1960), in which the field at great distance would seem to be dependent not only on the value of the time derivative of the field on a surface Σ, which we take to be the fracture surface of an elastic rupture but also on the spatial gradient of the slip. The Kirchhoff integration of the scalar wave equation is the more transparent and illustrative of the two. The solution to the scalar wave equation for radiation from sources on a closed surface Σ enclosing a volume V is (Stratton, 1941, p. 427, equation 22)

$$\psi(\mathbf{x},t)=\frac{1}{4\pi}\int_{\Sigma}\left\{\frac{1}{R}[\nabla\psi]-\frac{1}{R^2}[\psi]\boldsymbol{\gamma}-\frac{1}{cR}[\dot{\psi}]\boldsymbol{\gamma}\right\}\cdot\mathbf{n}(\boldsymbol{\xi})d\Sigma(\boldsymbol{\xi}),$$

where the brackets $[f(t)]$ denote time retardation by R/c, $[f(t)]=f(t-R/c)$; c is the wave velocity; the vector $\mathbf{R}$ extends from a point $\boldsymbol{\xi}$ on the surface to the point of observation at $\mathbf{x}$, $\mathbf{R}=\mathbf{x}-\boldsymbol{\xi}$, $R=|\mathbf{R}|$, and $\boldsymbol{\gamma}$ is the unit vector along $\mathbf{R}$, $\boldsymbol{\gamma}=\mathbf{R}/R$; $\mathbf{n}(\boldsymbol{\xi})$ is the outward drawn unit normal to the surface. The surface integral includes the contribution from sources outside V. If ψ and its spatial gradient and time derivative are known everywhere on Σ, ψ is completely determined at all interior points of the volume enclosed by Σ (provided that it is not possible to assign these values arbitrarily). In the far field the solution for the wave function includes the first and third of the terms just listed,

$$\psi(\mathbf{x},t)=\frac{1}{4\pi}\int_{\Sigma}\left\{\frac{1}{R}[\nabla\psi]-\frac{1}{cR}[\dot{\psi}]\boldsymbol{\gamma}\right\}\cdot\mathbf{n}(\boldsymbol{\xi})d\Sigma(\boldsymbol{\xi}).$$

The second of these latter terms is the expected, conventional component, which is proportional to its time derivative at the surface. The first term, which depends on the normal component of the spatial gradient on the surface, has been neglected in the treatment of radiation in the seismological literature to date.

In the elastic wave case Knopoff's solution (Knopoff, 1956, p. 223, equation 43) is quite complicated but consists of terms similar to those just discussed, which we do not re-

produce here for simplicity. The solution has two classes of terms with retardations having *P*- and *S*-wave velocities; each class includes terms with the two types of spatial (vector) differentiation (divergence and curl) and terms with the time derivative of the displacement on the surfaces. We refrain from being more explicit regarding the operators, which are relatively complex. Kirchhoff's solution for the scalar wave equation and Knopoff's solution for the elastic (vector) wave equation are for a one-sided surface. Though they are not given explicitly for the two-sided fault surface, they have the same essential properties, which is that their solutions consist not only of the wave function and its time derivative on the surface but also the vector spatial derivatives of the wave function (displacement). Our concern in this article is with the significance of the spatial derivative terms on a two-sided fault surface, which have been neglected heretofore. We give the solution to the elastic wave equation in a more useful form in the next section.

The familiar double-couple force equivalent (de Hoop, 1958, pp. 14–19; Knopoff and Gilbert, 1960; Maruyama, 1963; Burridge and Knopoff, 1964) is derivable directly from the properties of the terms in the time derivatives of the displacements. In this article we will show that the contribution of the spatial derivative of slip is indeed zero in the far field if the fault zone has zero thickness. However, it is nonzero if the fault zone has finite thickness, and there is a strength-weakening zone near an advancing crack tip. These hitherto neglected terms radiate as a single couple. The single-couple equivalent does not violate principles of Newtonian mechanics because the torque imbalance in the single couple is counterbalanced by rotations within the fault zone; the crack therefore radiates torque waves, which are shear waves manifested as a radiated rotational field at great distance.

Green's Function

Stokes' retarded solution (Stokes, 1849) for the Green's function G_{ij} for homogeneous elasticity in the far field is (Love, 1927, p. 305; Aki and Richards, 1980, p. 73)

$$4\pi\rho G_{ij} = \frac{\gamma_i\gamma_j}{\alpha^2 R}\delta\left(t-\tau-\frac{R}{\alpha}\right) + \frac{(\delta_{ij}-\gamma_i\gamma_j)}{\beta^2 R}\delta\left(t-\tau-\frac{R}{\beta}\right), \tag{1}$$

where the Green's function $G_{ij} = G_{ij}(\mathbf{x}, t; \boldsymbol{\xi}, \tau)$ is the displacement in the j direction at a distant point P($\mathbf{x}$) at time t due to a unit impulse in the i direction at Q($\boldsymbol{\xi}$) on a fault at time τ. ρ is the density of the medium, and α and β are the *P*- and *S*-wave velocities, respectively. We adopt the convention that the first index is the component of the force at the source, and the second is the component of the motion at (great) distance $R = |\mathbf{R}|$. The γ_is are the direction cosines of the vector $\mathbf{R} = \mathbf{x} - \boldsymbol{\xi}$ from an element of the source Q($\boldsymbol{\xi}$) to the point of observation P($\mathbf{x}$) (Fig. 1). We restrict the problem to the determination of the elastic wave radiation at P due to slip on the internal surface Σ.

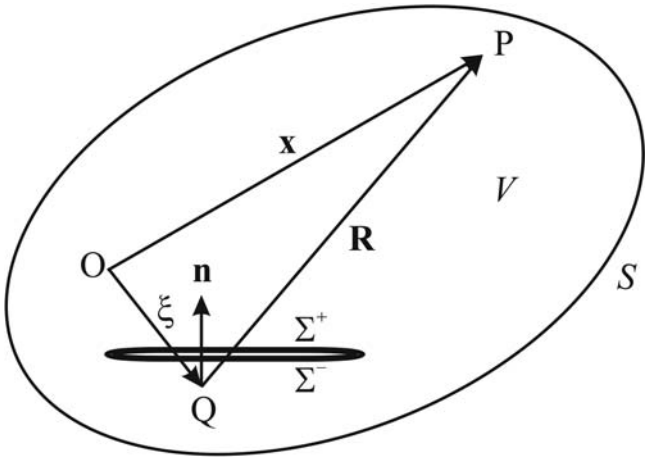

Figure 1. An elastic solid, with volume V and closed external and internal surfaces S and Σ, respectively. O is the origin of coordinates, P($\mathbf{x}$) is a point of observation within V, Q($\boldsymbol{\xi}$) is a slipping element on Σ, $n_k(\boldsymbol{\xi})$ is the outward drawn normal to surface Σ. The inner surface Σ has two nearby sheets Σ^+ and Σ^-.

The stress Green's function σ_{ijk} derived from equation (1) is

$$\sigma_{ijk} = \lambda\delta_{jk}G_{im,m} + \mu(G_{ij,k} + G_{ik,j}),$$

where λ and μ are the Lamé elastic parameters; we have dropped the arguments on σ_{ijk} and G_{ij}. From equation (1)

$$4\pi\rho\sigma_{ijk}(\mathbf{x}, t; \boldsymbol{\xi}, \tau) = -\frac{\gamma_i(\lambda\delta_{jk} + 2\mu\gamma_j\gamma_k)}{\alpha^3 R}\dot{\delta}\left(t-\tau-\frac{R}{\alpha}\right) - \frac{\mu(\psi_{ij}\gamma_k + \psi_{ik}\gamma_j)}{\beta^3 R}\dot{\delta}\left(t-\tau-\frac{R}{\beta}\right), \tag{2}$$

where $\psi_{ij} = \delta_{ij} - \gamma_i\gamma_j$ is a rotation operator, we use $\gamma_m\gamma_m = 1$, $\psi_{im}\gamma_m = 0$, and where we have differentiated only with respect to the second index in equation (1).

Integration of the Wave Equation

We consider sources only on the internal surface Σ. The wave equation for elasticity in the absence of body forces is

$$\tau_{jk,k} - \rho\ddot{u}_j = 0. \tag{3}$$

We solve (3) in a region V bounded by an extremely large outer surface S and the two surfaces of the zone of faulting, which is the internal surface Σ. The remoteness of S means that motions generated at Σ never reach S in time to influence the fields at P (Fig. 1). To solve (3) for slip on a fault, we let Σ have two sheets, Σ^+ and Σ^-, which are very close to one another. In what follows, we allow Σ^+ and Σ^- to have a small but finite separation.

The Green's function $G_{ij}(\mathbf{x}, t; \boldsymbol{\xi}, \tau)$ in equation (1) satisfies

$$\sigma_{ijk,k} - \rho\ddot{G}_{ij} = -\delta_{ij}\delta(\mathbf{x}-\boldsymbol{\xi})\delta(t-\tau), \tag{4}$$

where we have dropped the space and time arguments on σ_{ijk} and G_{ij}; $\sigma_{ijk} = \sigma_{ijk}(\mathbf{x}, t; \boldsymbol{\xi}, \tau)$ is the stress tensor Green's function in equation (2). In the usual way, multiply equation (3) by $G_{ij}(\mathbf{x}, t; \boldsymbol{\xi}, \tau)$ from equation (1), multiply equation (4) by $u_j(\boldsymbol{\xi}, \tau)$, and subtract. It follows that

$$\begin{aligned}(\tau_{jk,k}G_{ij} - u_j\sigma_{ijk,k}) - \rho(\ddot{u}_j G_{ij} - u_j\ddot{G}_{ij}) \\ = u_i\delta(\mathbf{x}-\boldsymbol{\xi})\delta(t-\tau).\end{aligned} \tag{5}$$

We integrate equation (5) over $V(\boldsymbol{\xi})$, $-\infty < \tau < \infty$, and apply Gauss' theorem. We obtain

$$u_i(\mathbf{x}, t) = \int_{-\infty}^{\infty} d\tau \int_{\Sigma} (u_j\sigma_{ijk} + \tau_{jk}G_{ij})n_k d\Sigma(\boldsymbol{\xi}), \tag{6}$$

where $u_j = u_j(\boldsymbol{\xi}, \tau)$, $\tau_{jk} = \tau_{jk}(\boldsymbol{\xi}, \tau)$, and $n_k = n_k(\boldsymbol{\xi})$ in the integrand. Equation (6) is the representation theorem for surface sources and is the point of departure for the remainder of this article.

The Usual Problem

We consider the first integral of equation (6),

$$u_i(\mathbf{x}, t) = \int_{-\infty}^{\infty} d\tau \int_{\Sigma} u_j\sigma_{ijk}n_k d\Sigma(\boldsymbol{\xi}). \tag{7}$$

We substitute the stress tensor Green's function σ_{ijk} from equation (2) into equation (7) and get the motion at P,

$$\begin{aligned}u_i(\mathbf{x}, t) = &-\int_{\Sigma} \frac{\gamma_i(\lambda\delta_{jk} + 2\mu\gamma_j\gamma_k)n_k}{4\pi\rho\alpha^3 R}\frac{\partial u_j(\boldsymbol{\xi}, t-\frac{R}{\alpha})}{\partial t}d\Sigma(\boldsymbol{\xi}) \\ &-\int_{\Sigma} \frac{\mu(\psi_{ij}\gamma_k + \psi_{ik}\gamma_j)n_k}{4\pi\rho\beta^3 R}\frac{\partial u_j(\boldsymbol{\xi}, t-\frac{R}{\beta})}{\partial t}d\Sigma(\boldsymbol{\xi}).\end{aligned} \tag{8}$$

We have used the identity

$$\int_{-\infty}^{\infty} u(\tau)\dot{\delta}\left(t-\tau-\frac{R}{\alpha}\right)d\tau = \dot{u}\left(t-\frac{R}{\alpha}\right).$$

The two terms in equation (8) have easily identifiable *P*- and *S*-wave retardations; we consider them separately.

Let the two sheets, Σ^+ and Σ^-, be separated by a small distance ΔW. It is easy to demonstrate that

$$\gamma_i^+ \approx \gamma_i^-\left\{1 + O\left(\frac{\Delta W}{R}\right)\right\}$$

$$\frac{1}{R^+} \approx \frac{1}{R^-}\left\{1 + O\left(\frac{\Delta W}{R}\right)\right\},$$

where R^+ is the distance R between a point $\boldsymbol{\xi}^+$ in the (upper) surface Σ^+ and the point of observation $\mathbf{x}$, which is therefore a function of $\boldsymbol{\xi}^+$. R^- is the same quantity for a point $\boldsymbol{\xi}^-$ in the (lower) surface Σ^-. If we neglect all terms of order higher than the zeroth in $\Delta W/R$ and notice that the two normals point in opposite directions $n_k^+ = -n_k^-$, we have

$$u_i^P(\mathbf{x}, t) = \int_{\Sigma} \frac{\gamma_i(\lambda\delta_{jk} + 2\mu\gamma_j\gamma_k)n_k}{4\pi\rho\alpha^3 R}\frac{\partial\langle u_j(\boldsymbol{\xi}, t-\frac{R}{\alpha})\rangle}{\partial t}d\Sigma(\boldsymbol{\xi})$$

$$u_i^S(\mathbf{x}, t) = \int_{\Sigma} \frac{\mu(\psi_{ij}\gamma_k + \psi_{ik}\gamma_j)n_k}{4\pi\rho\beta^3 R}\frac{\partial\langle u_j(\boldsymbol{\xi}, t-\frac{R}{\beta})\rangle}{\partial t}d\Sigma(\boldsymbol{\xi}),$$

where we now integrate only over one surface Σ^- of the two and drop the superscript, and $\langle u_j\rangle$ denotes the difference in the quantity in brackets across the fault zone. Let

$$\left\langle u_j\left(\boldsymbol{\xi}, t-\frac{R}{c}\right)\right\rangle = e_j\left\langle u\left(\boldsymbol{\xi}, t-\frac{R}{c}\right)\right\rangle,$$

where e_j is the unit vector in the direction of slip, and $\langle u\rangle$ is the jump in $u(\boldsymbol{\xi}, t-R/c)$ across the fault zone,

$$\left\langle u\left(\boldsymbol{\xi}, t-\frac{R}{c}\right)\right\rangle = u\left(\boldsymbol{\xi}^+, t-\frac{R^+}{c}\right) - u\left(\boldsymbol{\xi}^-, t-\frac{R^-}{c}\right).$$

Thus,

$$u_i^P(\mathbf{x}, t) = \int_{\Sigma} \frac{\gamma_i(\lambda\delta_{jk} + 2\mu\gamma_j\gamma_k)n_k e_j}{4\pi\rho\alpha^3 R}\frac{\partial\langle u(\boldsymbol{\xi}, t-\frac{R}{\alpha})\rangle}{\partial t}d\Sigma(\boldsymbol{\xi}) \tag{9.1}$$

$$u_i^S(\mathbf{x}, t) = \int_{\Sigma} \frac{\mu(\psi_{ij}\gamma_k + \psi_{ik}\gamma_j)n_k e_j}{4\pi\rho\beta^3 R}\frac{\partial\langle u(\boldsymbol{\xi}, t-\frac{R}{\beta})\rangle}{\partial t}d\Sigma(\boldsymbol{\xi}). \tag{9.2}$$

It is easy to show that

$$\begin{aligned}\left\langle u\left(\boldsymbol{\xi}, t-\frac{R}{c}\right)\right\rangle \approx &\Delta u\left(\boldsymbol{\xi}^-, t-\frac{R^-}{c}\right) \\ &+ \frac{\partial u(\boldsymbol{\xi}^-, t-\frac{R^-}{c})}{\partial t}\frac{\gamma_k^- n_k^-}{c}\Delta W\left\{1 + O\left(\frac{\Delta W}{cT_s}\right)\right\},\end{aligned} \tag{10}$$

where

$$\Delta u\left(\boldsymbol{\xi}^-, t-\frac{R^-}{c}\right) = u\left(\boldsymbol{\xi}^+, t-\frac{R^-}{c}\right) - u\left(\boldsymbol{\xi}^-, t-\frac{R^-}{c}\right)$$

is the usual jump in the displacement (dislocation) in $u(\boldsymbol{\xi}, t - R/c)$ across the fault zone at the same instant of time $t - R^-/c$, and T_s is the rise time, $c = \alpha$ or β.

It is worthy to note that the dislocation

$$\Delta u\left(\boldsymbol{\xi}^-, t - \frac{R^-}{c}\right) \approx D$$

and the slip velocity $\partial u(\boldsymbol{\xi}^-, t - R^-/c)/\partial t$ is related to the final slip D by

$$\frac{\partial u\left(\boldsymbol{\xi}^-, t - \frac{R^-}{c}\right)}{\partial t} \approx \frac{D/2}{T_s}.$$

Thus,

$$\left[u\left(\boldsymbol{\xi}, t - \frac{R}{c}\right)\right] \approx \Delta u\left(\boldsymbol{\xi}^-, t - \frac{R^-}{c}\right)\left[1 + O\left(\frac{\Delta W}{cT_s}\right)\right]. \tag{11}$$

Because the direction of slip e_j is perpendicular to the normal fault surface n_k for in-plane slip, $n_k e_k = 0$. Hence, equation (9) becomes

$$u_i^P(\mathbf{x}, t) = \int_\Sigma \frac{\beta^2 \gamma_i \gamma_j e_j \gamma_k n_k}{2\pi\alpha^3 R} \frac{\partial \Delta u(\boldsymbol{\xi}, t - \frac{R}{\alpha})}{\partial t} d\Sigma(\boldsymbol{\xi}), \tag{12.1}$$

$$u_i^S(\mathbf{x}, t) = \int_\Sigma \frac{(\psi_{ij}\gamma_k + \psi_{ik}\gamma_j) n_k e_j}{4\pi\beta R} \frac{\partial \Delta u(\boldsymbol{\xi}, t - \frac{R}{\beta})}{\partial t} d\Sigma(\boldsymbol{\xi}) \tag{12.2}$$

for in-plane slip. Equation (12) holds for the case of finite thickness of fault zone ΔW if $\Delta W/R \ll 1$ and $\Delta W/cT_s \ll 1$, where $c = \alpha$ or β. Equation (12) is formally in agreement with equation (14.6) of Aki and Richards (1980, p. 802) for the case of zero fault width. From the condition $\boldsymbol{\gamma} \times \boldsymbol{\gamma} = 0$ and the orthogonality condition $\gamma_i \psi_{ij} = 0$, we have that u_i^P and u_i^S are radially and transversely polarized with P-wave and S-wave retardations respectively. The radiation pattern $\gamma_j e_j \gamma_k n_k$ in equation (12.1) is the expected double-couple result for the P-wave radiation pattern.

For slip in the x_1 direction and the normal to Σ in the x_3 direction, in spherical polar coordinates (R, θ, ϕ) centered on the source,

$$\mathbf{e} = (1, 0, 0), \qquad \mathbf{n} = (0, 0, 1),$$
$$\boldsymbol{\gamma} = (\sin\theta\cos\phi, \sin\theta\sin\phi, \cos\theta),$$

measuring θ from the x_3 direction and taking the (x_1, x_3) plane as $\phi = 0$. Thus,

$$u_R^P(\mathbf{x}, t) = \int_\Sigma \frac{\beta^2 \sin 2\theta \cos\phi}{4\pi\alpha^3 R} \frac{\partial \Delta u(\boldsymbol{\xi}, t - \frac{R}{\alpha})}{\partial t} d\Sigma(\boldsymbol{\xi}). \tag{13.1}$$

We also calculate the amplitude of the S-wave term. The S-wave terms in the θ and ϕ directions are

$$u_\theta^S(\mathbf{x}, t) = \int_\Sigma \frac{\cos 2\theta \cos\phi}{4\pi\beta R} \frac{\partial \Delta u(\boldsymbol{\xi}, t - \frac{R}{\beta})}{\partial t} d\Sigma(\boldsymbol{\xi}), \tag{13.2}$$

$$u_\phi^S(\mathbf{x}, t) = -\int_\Sigma \frac{\cos\theta \sin\phi}{4\pi\beta R} \frac{\partial \Delta u(\boldsymbol{\xi}, t - \frac{R}{\beta})}{\partial t} d\Sigma(\boldsymbol{\xi}). \tag{13.3}$$

In the (x_1, x_3) plane ($u_\phi^S = 0$), u_θ^S is the expected quadrifoliate radiation pattern rotated by 45° from the P-wave pattern in the double-couple case.

This concludes our treatment of the usual term. This part of the result, the double-couple force equivalent, holds whether we have a strength-weakening zone or not because the first term of equation (6) does not depend on the stresses. In this case the far-field radiation is proportional to the slip velocity on the fault and is the canonical result. The ratio of the amplitudes of the P- and S-wave terms is $(\beta/\alpha)^3$ except for the angular polarization coefficients.

The Strength-Weakening Zone

We return to the problem of the second term in the integral of equation (6). As remarked, this term is zero if $\langle \tau_{jk}(\boldsymbol{\xi}, \tau) \rangle = \tau_{jk}(\boldsymbol{\xi}^+, \tau) - \tau_{jk}(\boldsymbol{\xi}^-, \tau) = 0$. In this case, the only term in the solution is the conventional double couple of the preceding section. However, in a strength-weakening zone (such as near the edge of an advancing crack), the stress is time-dependent and nonzero because the stress drop must vary between the critical shear stress and its final value at the edge of the strength-weakening zone (Fig. 2). The terms $\tau_{jk} n_k$ are the tractions on the two surfaces; they are oppositely directed and each nonzero. Thus, the radiation from the nucleation site and from the evolution of the crack at its edge

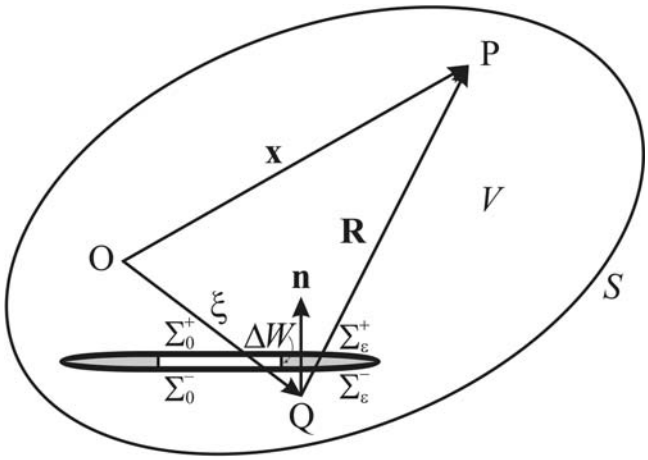

Figure 2. An elastic solid with volume V, closed external surface S, and an internal surface $\Sigma = \Sigma_0 + \Sigma_\varepsilon$. The internal surface consists of the dislocation surface $\Sigma_0 = \Sigma_0^+ + \Sigma_\varepsilon^-$ and the surface of the strength-weakening zone (area in light gray) $\Sigma_\varepsilon = \Sigma_\varepsilon^+ + \Sigma_\varepsilon^-$. ΔW is the thickness of the strength-weakening zone, O is the origin of coordinates, P($\mathbf{x}$) is a point of observation within V, Q($\boldsymbol{\xi}$) is a slipping element on Σ_ε, $n_k(\boldsymbol{\xi})$ is the outward drawn normal to surface Σ.

must have a component that depends on the stress in these regions. The mathematical problem is simpler than that of the preceding section.

In this problem we start with

$$u_i(\mathbf{x},t)=\int_{-\infty}^{\infty}d\tau\int_{\Sigma_\varepsilon}G_{ij}\tau_{jk}n_k d\Sigma(\boldsymbol{\xi}) \tag{14}$$

from equation (6), where Σ_ε is the surface of the strength-weakening zone. From equation (1)

$$u_i(\mathbf{x},t)=\int_{-\infty}^{\infty}d\tau\int_{\Sigma_\varepsilon}\left\{\frac{\gamma_i\gamma_j}{4\pi\rho\alpha^2R}\delta\left(t-\tau-\frac{R}{\alpha}\right)+\frac{(\delta_{ij}-\gamma_i\gamma_j)}{4\pi\rho\beta^2R}\delta\left(t-\tau-\frac{R}{\beta}\right)\right\}\tau_{jk}(\boldsymbol{\xi},\tau)n_k d\Sigma(\boldsymbol{\xi}).$$

As before the *P*-wave term is radially polarized, and the *S*-wave terms are orthogonally polarized to the *P* waves. The two terms are

$$u_i^P(\mathbf{x},t)=\int_{\Sigma_\varepsilon}\frac{\gamma_i\gamma_j}{4\pi\rho\alpha^2R}\tau_{jk}\left(\boldsymbol{\xi},t-\frac{R}{\alpha}\right)n_k d\Sigma(\boldsymbol{\xi}) \tag{15.1}$$

$$u_i^S(\mathbf{x},t)=\int_{\Sigma_\varepsilon}\frac{(\delta_{ij}-\gamma_i\gamma_j)}{4\pi\rho\beta^2R}\tau_{jk}\left(\boldsymbol{\xi},t-\frac{R}{\beta}\right)n_k d\Sigma(\boldsymbol{\xi}). \tag{15.2}$$

Let $\tau_{jk}(\boldsymbol{\xi},t)n_k=e_jT(\boldsymbol{\xi},t)$, where $e_jT(\boldsymbol{\xi},t)$ is the traction acting on the surface element $d\Sigma$ having the outward drawn unit normal n_k, e_j is the unit vector in the direction of the traction. Thus,

$$u_i^P(\mathbf{x},t)=\int_{\Sigma_\varepsilon}\frac{\gamma_i\gamma_j e_j}{4\pi\rho\alpha^2R}T\left(\boldsymbol{\xi},t-\frac{R}{\alpha}\right)d\Sigma(\boldsymbol{\xi}) \tag{16.1}$$

$$u_i^S(\mathbf{x},t)=\int_{\Sigma_\varepsilon}\frac{(\delta_{ij}-\gamma_i\gamma_j)e_j}{4\pi\rho\beta^2R}T\left(\boldsymbol{\xi},t-\frac{R}{\beta}\right)d\Sigma(\boldsymbol{\xi}). \tag{16.2}$$

We take the conditions just presented, that is, $\mathbf{e}=(1,0,0)$, $\mathbf{n}=(0,0,1)$,$\boldsymbol{\gamma}=(\sin\theta\cos\phi,\sin\theta\sin\phi,\cos\theta)$. The *P*-wave term is

$$u_R^P(\mathbf{x},t)=\int_{\Sigma_\varepsilon}\frac{\sin\theta\cos\phi}{4\pi\rho\alpha^2R}T\left(\boldsymbol{\xi},t-\frac{R}{\alpha}\right)d\Sigma(\boldsymbol{\xi}). \tag{17.1}$$

The *S*-wave terms are

$$u_\theta^S(\mathbf{x},t)=\int_{\Sigma_\varepsilon}\frac{\cos\theta\cos\phi}{4\pi\rho\beta^2R}T\left(\boldsymbol{\xi},t-\frac{R}{\beta}\right)d\Sigma(\boldsymbol{\xi}), \tag{17.2}$$

$$u_\phi^S(\mathbf{x},t)=-\int_{\Sigma_\varepsilon}\frac{\sin\phi}{4\pi\rho\beta^2R}T\left(\boldsymbol{\xi},t-\frac{R}{\beta}\right)d\Sigma(\boldsymbol{\xi}). \tag{17.3}$$

The integrands are the radiation from a point force in the x_1 direction.

In equation (15) if we take the contribution from the internal surfaces $\Sigma_\varepsilon=\Sigma_\varepsilon^+ + \Sigma_\varepsilon^-$ into account, the point sources point in opposite directions, and we have a vector point pointing in the e_j direction plus a couple of oppositely directed forces separated by a distance equal to the thickness of the fault. This is a torque whose axis of rotation points is in the $\mathbf{e}\times\mathbf{n}$ direction (i. e., a single couple).

Let $\tau_{jk}(\boldsymbol{\xi},t)n_k=e_jT(\boldsymbol{\xi},t)$ and $n_k^+=-n_k^-$ show as before. From equation (15) we have

$$u_i^P(\mathbf{x},t)=-\int_{\Sigma_\varepsilon}\frac{\gamma_i\gamma_j e_j}{4\pi\rho\alpha^2R}\left\langle T\left(\boldsymbol{\xi},t-\frac{R}{\alpha}\right)\right\rangle d\Sigma(\boldsymbol{\xi}) \tag{18.1}$$

$$u_i^S(\mathbf{x},t)=-\int_{\Sigma_\varepsilon}\frac{(\delta_{ij}-\gamma_i\gamma_j)e_j}{4\pi\rho\beta^2R}\left\langle T\left(\boldsymbol{\xi},t-\frac{R}{\beta}\right)\right\rangle d\Sigma(\boldsymbol{\xi}) \tag{18.2}$$

as $\Delta W/R\ll 1$, where we now integrate over only the lower surface and drop the superscript. In equation (18) $\langle T(\boldsymbol{\xi},t-R/c)\rangle$ is the jump in $T(\boldsymbol{\xi},t-R/c)$ across the fault zone of thickness ΔW,

$$\left\langle T\left(\boldsymbol{\xi},t-\frac{R}{c}\right)\right\rangle=T\left(\boldsymbol{\xi}^+,t-\frac{R^+}{c}\right)-T\left(\boldsymbol{\xi}^-,t-\frac{R^-}{c}\right).$$

It is easy to show that

$$\left\langle T\left(\boldsymbol{\xi},t-\frac{R}{c}\right)\right\rangle\approx\Delta T\left(\boldsymbol{\xi}^-,t-\frac{R^-}{c}\right)+\frac{\partial T(\boldsymbol{\xi}^-,t-\frac{R^-}{c})}{\partial t}\frac{\gamma_k^-n_k^-}{c}\Delta W\left\{1+O\left(\frac{\Delta W}{cT_s'}\right)\right\}, \tag{19}$$

where

$$\Delta T\left(\boldsymbol{\xi}^-,t-\frac{R^-}{c}\right)=T\left(\boldsymbol{\xi}^+,t-\frac{R^-}{c}\right)-T\left(\boldsymbol{\xi}^-,t-\frac{R^-}{c}\right)$$

is the stress dislocation, and T_s' is the characteristic time for stress change, $c=\alpha$ or β.

Although equations (10) and (19) are similar in form, they are essentially quite different. Unlike equation (10), where $\Delta u(\boldsymbol{\xi}^-,t-R^-/c)$ and $\partial u(\boldsymbol{\xi}^-,t-R^-/c)/\partial t$ are related due to the fact that $\Delta u(\boldsymbol{\xi}^-,t-R^-/c)\approx D$ and $\partial u(\boldsymbol{\xi}^-,t-R^-/c)/\partial t\approx D/2T_s$ in equation (19) $\Delta T(\boldsymbol{\xi}^-,t-R^-/c)$ is the stress dislocation while $\partial T(\boldsymbol{\xi}^-,t-R^-/c)/\partial t$ is the time rate of stress; the latter quantities are not related as they are in the displacement dislocation case. The stress dislocation $\Delta T(\boldsymbol{\xi}^-,t-R^-/c)$ may be zero or a certain finite quantity, regardless of whether the thickness of the fault zone is finite or zero. There is no similar relationship relating the stress dislocation $\Delta T(\boldsymbol{\xi}^-,t-R^-/c)$ with the time rate of

stress $\partial T(\boldsymbol{\xi}^-, t - R^-/c)/\partial t$ such as $\Delta u(\boldsymbol{\xi}^-, t - R^-/c) \approx D$ and $\partial u(\boldsymbol{\xi}^-, t - R^-/c)/\partial t \approx D/2T_s$.

In the case $\Delta W/R \ll 1$, $\Delta W/cT_s \ll 1$ and $\Delta W/cT_s' \ll 1$, where $c = \alpha$ or β, we have

$$\left\langle u\left(\boldsymbol{\xi}, t - \frac{R}{c}\right)\right\rangle \approx \Delta u\left(\boldsymbol{\xi}^-, t - \frac{R^-}{c}\right) \tag{20}$$

and

$$\left\langle T\left(\boldsymbol{\xi}, t - \frac{R}{c}\right)\right\rangle \approx \Delta T\left(\boldsymbol{\xi}^-, t - \frac{R^-}{c}\right) + \frac{\partial T(\boldsymbol{\xi}^-, t - \frac{R^-}{c})}{\partial t}\frac{\gamma_k^- n_k^-}{c}\Delta W. \tag{21}$$

The second term of the right-hand side of equation (21) cannot be neglected although the second term of the right-hand side of equation (10) can be in the case of $\Delta W/R \ll 1$, $\Delta W/cT_s \ll 1$, and $\Delta W/cT_s' \ll 1$. The difference in the two cases arises because the first term in equation (10) is nonzero and persists as $\Delta W \to 0$, while in the case of equation (21), the first term may be zero if the stress drop is continuous across the fault zone.

The first term on the right-hand side of equation (21) contributes the usual solution for a stress dislocation,

$$u_i^P(\mathbf{x}, t) = -\int_{\Sigma_\varepsilon} \frac{\gamma_i\gamma_j e_j}{4\pi\rho\alpha^2 R}\Delta T\left(\boldsymbol{\xi}, t - \frac{R}{\alpha}\right)d\Sigma(\boldsymbol{\xi}), \tag{22.1}$$

$$u_i^S(\mathbf{x}, t) = -\int_{\Sigma_\varepsilon} \frac{(\delta_{ij} - \gamma_i\gamma_j)e_j}{4\pi\rho\beta^2 R}\Delta T\left(\boldsymbol{\xi}, t - \frac{R}{\beta}\right)d\Sigma(\boldsymbol{\xi}). \tag{22.2}$$

As in equation (16) this is the radiation from a point source of strength of $-\Delta T$ pointing in the e_j direction. The solution for the stress dislocation is zero if the traction on Σ_ε is continuous.

The second term of the right-hand side of equation (21) is the solution for a single couple of oppositely directed, time-dependent forces separated by a distance equal to the thickness of the fault and is nonzero even if the traction is continuous across the fault,

$$u_i^P(\mathbf{x}, t) = -\int_{\Sigma_\varepsilon} \frac{\gamma_i\gamma_j e_j\gamma_k n_k}{4\pi\rho\alpha^3 R}\Delta W\frac{\partial T(\boldsymbol{\xi}, t - \frac{R}{\alpha})}{\partial t}d\Sigma(\boldsymbol{\xi}), \tag{23.1}$$

$$u_i^S(\mathbf{x}, t) = -\int_{\Sigma_\varepsilon} \frac{(\delta_{ij} - \gamma_i\gamma_j)e_j\gamma_k n_k}{4\pi\rho\beta^3 R}\Delta W\frac{\partial T(\boldsymbol{\xi}, t - \frac{R}{\beta})}{\partial t}d\Sigma(\boldsymbol{\xi}), \tag{23.2}$$

where ΔW is the thickness of the strength-weakening zone, $-\partial T/\partial t$ is the time rate of stress-drop increase, and the integration takes place only over the lower surface of the strength-weakening zone. Equation (23) holds for similar conditions as equation (12) for the case of finite thickness of fault zone ΔW if $\Delta W/R \ll 1$ and $\Delta W/cT_s' \ll 1$, where $c = \alpha$ or β.

For the same conditions listed in the previous paragraph, that is, $\mathbf{e} = (1, 0, 0)$, $\mathbf{n} = (0, 0, 1)$, $\boldsymbol{\gamma} = (\sin\theta\cos\phi, \sin\theta\sin\phi, \cos\theta)$, the P-wave term is

$$u_R^P(\mathbf{x}, t) = -\int_{\Sigma_\varepsilon} \frac{\sin 2\theta\cos\phi}{8\pi\rho\alpha^3 R}\Delta W\frac{\partial T(\boldsymbol{\xi}, t - \frac{R}{\alpha})}{\partial t}d\Sigma(\boldsymbol{\xi}), \tag{24.1}$$

the S-wave terms in the θ and ϕ directions are

$$u_\theta^S(\mathbf{x}, t) = -\int_{\Sigma_\varepsilon} \frac{\cos^2\theta\cos\phi}{4\pi\rho\beta^3 R}\Delta W\frac{\partial T(\boldsymbol{\xi}, t - \frac{R}{\beta})}{\partial t}d\Sigma(\boldsymbol{\xi}), \tag{24.2}$$

$$u_\phi^S(\mathbf{x}, t) = \int_{\Sigma_\varepsilon} \frac{\cos\theta\sin\phi}{4\pi\rho\beta^3 R}\Delta W\frac{\partial T(\boldsymbol{\xi}, t - \frac{R}{\beta})}{\partial t}d\Sigma(\boldsymbol{\xi}). \tag{24.3}$$

This is the radiation from a single couple with time-dependent forces in the $\pm x_1$ direction and torque axis in the x_3 direction. The solution, which gives a time-dependent single couple, is consistent with that obtained by Knopoff and Gilbert (1960) for the problem of radiation from a fault of finite thickness with stress drop across the fault.

The solution for the radiation from a strength-weakening zone depends on the rate of stress drop. A comparison between equations (12) and (23) or (13) and (24) shows that the expressions for the radiation from an element of the strength-weakening zone are equivalent to the radiation from a single couple with torque, while the radiation from an element of slip is equivalent to the radiation from a double couple without torque. They have opposite signs, expressing the fact that the radiation from the strength-weakening zone arises from the varying (decreasing) stress within the strength-weakening zone, which is opposite to the direction of the increasing stress drop before breakdown, while the radiation from the completely fractured crack is a consequence of the breakdown of the weakening zone and the increasing dislocation.

Torque Waves

The radiation of a torque wave is part of the deformation field, which results from the relative displacement (Bullen, 1953, pp. 13–14). Consider an element of solid material within which displacements $\mathbf{u}(\mathbf{x})$ have occurred. Let the particle initially at position $\mathbf{x}$ be moved to position $\mathbf{x} + \mathbf{u}(\mathbf{x})$. The displacement of a point at position $\mathbf{x} + \delta\mathbf{x}$ is

$$u_i(\mathbf{x} + \delta\mathbf{x}) \approx u_i(\mathbf{x}) + \frac{\partial u_i(\mathbf{x})}{\partial x_j}\delta x_j, \tag{25}$$

where $\delta\mathbf{x}$ is infinitesimal and where the partial derivatives are evaluated at $\mathbf{x}$. By adding and subtracting $(1/2)(\partial u_j(\mathbf{x})/\partial x_i)\delta x_j$ to equation (25), the displacement of the point at $\mathbf{x}+\delta\mathbf{x}$ can be separated into three parts

$$u_i(\mathbf{x}+\delta\mathbf{x}) \approx u_i(\mathbf{x}) + e_{ij}\delta x_j - \omega_{ij}\delta x_j, \tag{26}$$

where e_{ij} is the symmetric strain tensor, and ω_{ij} is the antisymmetric rotation tensor

$$e_{ij} = \frac{1}{2}\left(\frac{\partial u_j}{\partial x_i} + \frac{\partial u_i}{\partial x_j}\right), \omega_{ij} = \frac{1}{2}\left(\frac{\partial u_j}{\partial x_i} - \frac{\partial u_i}{\partial x_j}\right).$$

The rotation tensor can be written as

$$-\omega_{ij}\delta x_j = (\boldsymbol{\Omega}\times\delta\mathbf{x})_i, \tag{27.1}$$

$$\boldsymbol{\Omega} = \frac{1}{2}\nabla\times\mathbf{u}, \tag{27.2}$$

where $\boldsymbol{\Omega}$ is the rotation vector.

The elastic wave equation (3) for homogeneous elasticity is

$$(\lambda+2\mu)\nabla(\nabla\cdot\mathbf{u}) - \mu\nabla\times(\nabla\times\mathbf{u}) = \rho\ddot{\mathbf{u}} - \mathbf{f} \tag{28}$$

for which equation (6) is the solution. We take the curl of equation (28) and get

$$\mu\nabla^2\boldsymbol{\Omega} = \rho\ddot{\boldsymbol{\Omega}} - \frac{1}{2}\nabla\times\mathbf{f}.$$

Hence, the rotations are S waves and can be expected to be orthogonal to both the P- and, via equation (27.2), the S-wave components of the motion.

Equation (26) shows that in an elastic solid, the deformation in the vicinity of $\mathbf{x}$ consists of three parts. The first part, which is given by the first term of equation (26) ($u_i(\mathbf{x})$), is equal to the displacement of $\mathbf{x}$ and thus, corresponds to a pure translation of matter near $\mathbf{x}$, which produces no deformation or rotation. The second part, represented by the e_{ij} term, is the true elastic distortion resulting from the differential motion within the body. The third part, represented by the $\boldsymbol{\Omega}$ term, corresponds to the pure rotation of a small volume element containing the point $\mathbf{x}$ about an axis parallel to $\boldsymbol{\Omega}$. This is a local rotation and should not be confused with the rigid rotation of the whole body, which has been excluded from $\mathbf{u}$ *ab initio* or with the microscopic rotational motion in which a typical particle is considered not as a material point but as an infinitesimal rigid body (Nowacki, 1986, p. 9).

In the case of in-plane slip the $u_i^P(\mathbf{x},t)$ term in the far field of equation (12.1) is irrotational and makes no contribution to rotational motion, while the $u_i^S(\mathbf{x},t)$ term of equation (12.2) is rotational and contributes rotational waves or torque-waves

$$\Omega_i(\mathbf{x},t) = -\int_\Sigma \frac{\varepsilon_{ikl}\gamma_j\gamma_k(n_j e_l + e_j n_l)}{8\pi\beta^2 R}\frac{\partial^2\Delta u(\boldsymbol{\xi}, t-\frac{R}{\beta})}{\partial t^2}d\Sigma(\boldsymbol{\xi}), \tag{29}$$

where ε_{ikl} is the usual permutation symbol.

From equation (29) the far-field rotational waves or torque waves for in-plane slip depend on the slip acceleration on the fault. From the orthogonality condition that $\gamma_i\Omega_i = 0$ and equation (29), we have that the rotation is orthogonal to both the P-wave motions $u_i^P(\mathbf{x},t)$ and the S-wave motions $u_i^S(\mathbf{x},t)$ and travels with S-wave velocity.

For the coordinate system just presented, that is, $\mathbf{e} = (1,0,0)$, $\mathbf{n} = (0,0,1)$, $\boldsymbol{\gamma} = (\sin\theta\cos\phi, \sin\theta\sin\phi, \cos\theta)$, the rotational or torque waves from a double-couple source are

$$\Omega_R(\mathbf{x},t) = 0, \tag{30.1}$$

$$\Omega_\theta(\mathbf{x},t) = -\int_\Sigma \frac{\cos\theta\sin\phi}{8\pi\beta^2 R}\frac{\partial^2\Delta u(\boldsymbol{\xi}, t-\frac{R}{\beta})}{\partial t^2}d\Sigma(\boldsymbol{\xi}), \tag{30.2}$$

$$\Omega_\phi(\mathbf{x},t) = -\int_\Sigma \frac{\cos 2\theta\cos\phi}{8\pi\beta^2 R}\frac{\partial^2\Delta u(\boldsymbol{\xi}, t-\frac{R}{\beta})}{\partial t^2}d\Sigma(\boldsymbol{\xi}). \tag{30.3}$$

Equation (30) is in agreement with the far-field term of equation (30) obtained by Cochard *et al.* (2006).

As in the case of in-plane slip (i.e., the case of a double-couple source), in the case of time-dependent stress drop in the strength-weakening zone, which is the case of a single couple, the $u_i^P(\mathbf{x},t)$ term expressed by equation (23.1) makes no contribution in the far field to rotational motions. The $u_i^S(\mathbf{x},t)$ term expressed in (23.2) contributes rotational waves

$$\Omega_i(\mathbf{x},t) = \int_{\Sigma_\varepsilon} \frac{\varepsilon_{ikl}\gamma_k e_l\gamma_j n_j}{8\pi\beta^2 R}\Delta W\frac{\partial^2 T(\boldsymbol{\xi}, t-\frac{R}{\beta})}{\partial t^2}d\Sigma(\boldsymbol{\xi}). \tag{31}$$

The far-field rotational waves or torque waves from the stress drop in the strength-weakening zone depend on the stress acceleration $\partial^2 T/\partial t^2$ in the fault plane. In this case of strength weakening from the orthogonality condition $\gamma_i\Omega_i = 0$ and equation (31), we have that Ω_i is orthogonal to both the P-wave motions $u_i^P(\mathbf{x},t)$ and S-wave motions $u_i^S(\mathbf{x},t)$ and with S-wave retardation in the far field.

Under the same conditions presented in the last paragraph $\mathbf{e} = (1,0,0)$, $\mathbf{n} = (0,0,1)$, $\boldsymbol{\gamma} = (\sin\theta\cos\phi, \sin\theta\sin\phi, \cos\theta)$, the rotation from the single-couple source is

$$\Omega_R(\mathbf{x},t) = 0, \tag{32.1}$$

$$\Omega_\theta(\mathbf{x}, t) = \int_{\Sigma_\varepsilon} \frac{\cos\theta \sin\phi}{8\pi\beta^2 R} \Delta W \frac{\partial^2 T(\boldsymbol{\xi}, t - \frac{R}{\beta})}{\partial t^2} d\Sigma(\boldsymbol{\xi}), \quad (32.2)$$

$$\Omega_\phi(\mathbf{x}, t) = \int_{\Sigma_\varepsilon} \frac{\cos^2\theta \cos\phi}{8\pi\beta^2 R} \Delta W \frac{\partial^2 T(\boldsymbol{\xi}, t - \frac{R}{\beta})}{\partial t^2} d\Sigma(\boldsymbol{\xi}). \quad (32.3)$$

Seismic Effects of Finite Fault Thickness

The presence of a single-couple source is not in conflict with the usual interpretation of double-couple force equivalents: the double couple is the lowest order combination of forces, which has no net force and no torque. How then can we have a single-couple solution in this case? The answer comes from an appreciation of the fact that our fault has a finite thickness and that the relaxation of static torques within the fault zone is exactly compensated by the radiation of torque waves from the fault. The double-couple solution is the appropriate solution if the fault has zero thickness (Fig. 3). If the fault zone has zero thickness, the torque, which is equal to the product of the traction and fault thickness, is zero. During an earthquake event, a transition zone, also known as a breakdown or cohesive zone, is found at the edge of the crack. Within this zone the medium undergoes a gradual transition from the continuum state of static elasticity to the nonlinear ruptured state. The stress across the fault plane is related to the slip by the constitutive relation, as shown schematically in Figure 4 (Ohnaka and Yamashita, 1989; Ohnaka *et al.* (1997); Venkataraman and Kanamori, 2004). In this figure, σ_0 is the initial stress or prestress (i.e., the stress before the earthquake or the stress in the surrounding medium). σ_p is the yield stress or peak strength (i.e., the upper limit of static frictional stress). At this level instantaneous instability begins, and strength weakening occurs; σ_d is the dynamic frictional stress, and σ_1 is the final or static frictional stress.

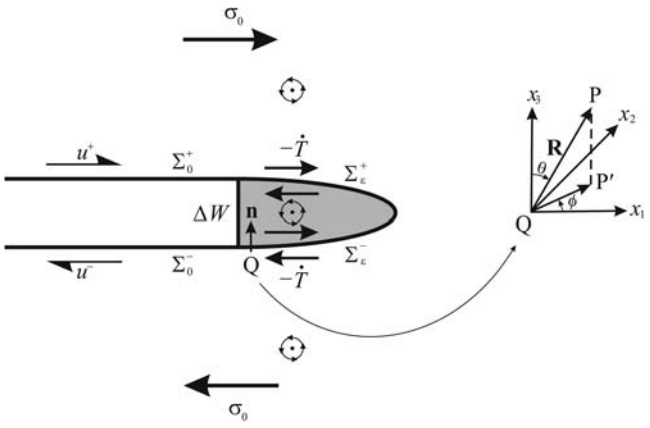

Figure 3. Radiation from a strength-weakening zone of a finite thickness of ΔW is equivalent to a single couple. $-\dot{T}$ is the time rate of increase of stress drop. The axis of rotation for the torque exerted by $-\dot{T}$ points in the $-\mathbf{e} \times \mathbf{n}$ direction (x_2 direction in the present example). This radiation of torque wave (small circles rotated counterclockwise outside the strength-weakening zone) from the fault exactly compensates the relaxation of torques within the fault and points in the $\mathbf{e} \times \mathbf{n}$ direction (negative x_2 direction in the present example) as schematically shown by the single couple and the small circle rotated counterclockwise within the strength-weakening zone. The figure to the right represents the spherical polar coordinate system centered at a slipping element $Q(\boldsymbol{\xi})$ on Σ_ε (not to scale). P is a point of observation, P′ is the projection of P onto the (x_1, x_2) plane. For explanation of the other symbols, see text. The net force, which is the sum of the tractions T, may be zero, but nevertheless they exert a torque because of the finite separation.

With this constitutive relation we can analyze the moment release in dynamic earthquake ruptures. Let us assume that a dynamically ruptured fault propagates with variable rupture velocity v_f in the x_1 direction (see Fig. 5c). In the elastic solid, dynamical rupture will initiate at a point where the strength excess is least; after initiation a stress concentration is located at the crack tip. The shear stress on the fault plane ($x_3 = 0$) far ahead of the crack tip is the initial stress σ_0. The shear stress σ rises from the initial stress σ_0 to the yield stress or peak strength σ_p and then decreases to the dynamic frictional stress σ_d (Fig. 5a). During the slip-weakening part of the process, the shear stress drops from σ_p to the dynamical frictional stress σ_d with continuing, increasing slip. The critical slip D_c marks the transition from the decreasing stress to the steady, dynamical friction. Slip continues to the final slip D resisted by the dynamic sliding friction σ_d where healing begins (Fig. 5b). When the slip stops the stress on the newly locked portion of the fault continues to vary (increase) with time, ultimately approaching the final (static) frictional stress σ_1. σ_1 may be greater than, equal to, or smaller than σ_d, but in Figures 4 and 5 only the case $\sigma_1 > \sigma_d$ is shown for simplicity.

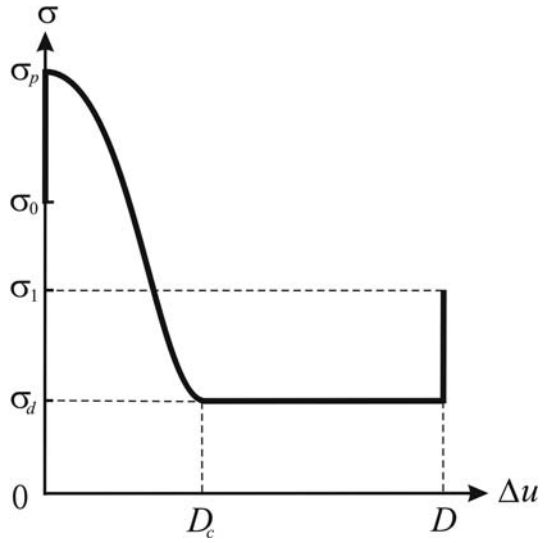

Figure 4. Constitutive relation of shear stress across the fault plane versus slip (after Ohnaka and Yamashita, 1989; Ohnaka *et al.*, 1997; Venkataraman and Kanamori, 2004).

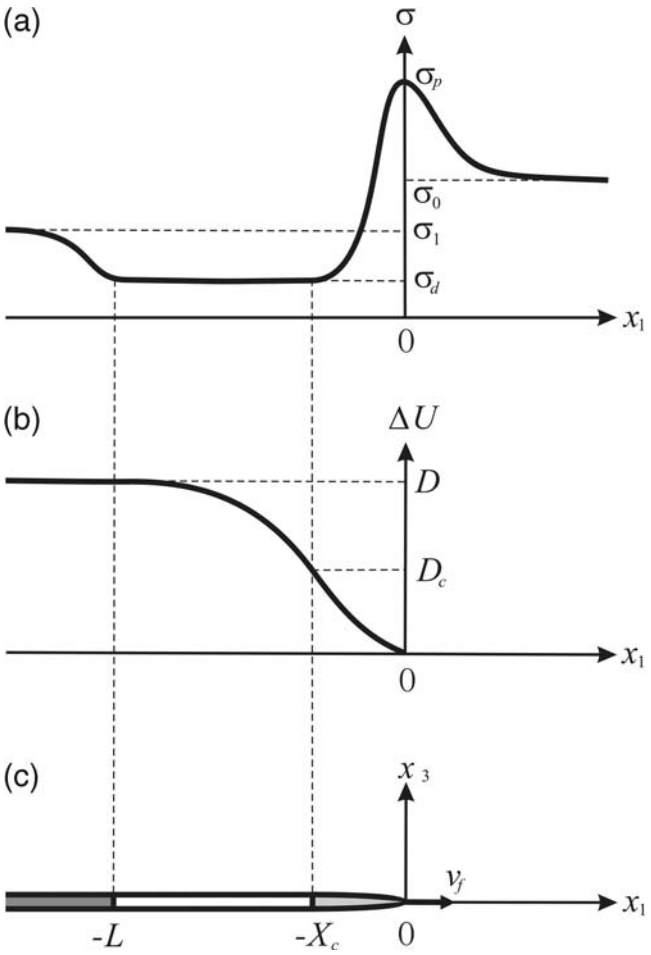

Figure 5. Distribution of stress (a) and slip (b) within the breakdown zone for a dynamically ruptured fault (c). Area in light gray ($-X_c \le x_1 \le 0$) represents the breakdown zone, and area in dark gray ($x_1 \le -L$) represents the healing portion of the fault (after Heaton, 1990; Rice *et al.*, 2005). For explanations of other symbols, see text. The patterns in this figure travel rightward.

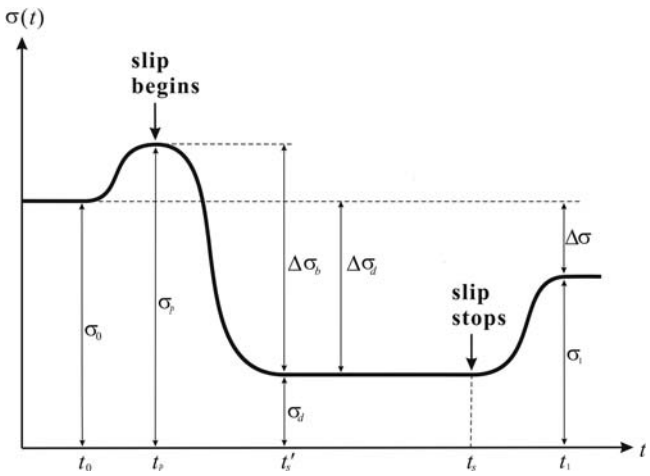

Figure 6. Time dependence of stress at a representative point on the fault plane. For explanation of the symbols, see text (after Yamashita, 1976).

In contrast to Figure 5, which presented a picture in space of the variations in stress, Figure 6 illustrates schematically the stress change with time at a representative point on the fault plane (Yamashita, 1976) as the stress-change pattern associated with crack growth moves across the point. At time t_0 rupture initiates at the hypocenter on the fault plane. As rupture progresses from the point of initiation to this point, the stress begins to increase from σ_0 to peak stress σ_p at time t_p. As slip increases from zero to D_c, strength-weakening occurs, and stress drops from σ_p to the dynamic frictional stress σ_d at time t_s'. For slip greater than D_c, the stress on the fault plane is σ_d until the slip comes to a stop at time t_s. D_c is the breakdown slip or critical slip-weakening distance. After the slip stops, the stress increases to the final stress σ_1 at time t_1. Our concern in this article has been with the time-dependent stress during the slip-weakening process. In addition to the increase in slip, which accompanies the stress decrease in the early stages of fracturing, there is an increase of stress (as noted in Fig. 6), which takes place in the example of the figure after the slip stops. If the increase in stress takes place before slip stops completely, there will be a contribution to the single-component term from the stopping phase. In this article we consider only the first of the two episodes of single-couple radiation and assume that strength hardening takes place only after all slip has been completed and is nonradiative.

We do not enter into present day arguments concerning the cause of the stoppage of slip in self-healing pulses, whether it is due to an increase of sliding friction as slip decelerates (Heaton, 1990; Cochard and Madariaga, 1996; Zheng and Rice, 1998) or due to an encounter of the crack with an extended strong region in the fault surface, which is a region of high strength excess (Mikumo and Miyatake, 1978; Day, 1982; Wald and Heaton, 1994), and which causes the increase in the friction in Figure 6. As in Figures 4 and 5, only the case of $\sigma_1 > \sigma_d$ is shown in Figure 6. $\Delta\sigma_b = \sigma_p - \sigma_d$ is the effective shear stress. $\Delta\sigma_d = \sigma_0 - \sigma_d$ is the dynamic stress drop, and $\Delta\sigma = \sigma_0 - \sigma_1$ is the static stress drop. Thus, the breakdown zone is a zone within which the stress changes dramatically.

On a ruptured portion of the fault of area ΔA, the far-field radiation due to the increase of the stress drop is approximately proportional to the time rate of torque moment (equation 23)

$$\Delta\dot{M}_t = \Delta W \Delta\dot{\sigma} \Delta A, \tag{33}$$

where ΔW is the thickness of the breakdown zone, $\Delta\dot{\sigma}$ is the time rate of increase of effective shear stress $\Delta\sigma(t)$ (i.e., the rate of increase of the stress drop),

$$\Delta\sigma(t) = \sigma_p - \sigma(t) \tag{34}$$

$\sigma(t)$ is the shear stress as a function of time. From the integration of $\Delta\dot{M}_t$ over the complete time of fracture and the entire fractured area, we get the total torque moment release

$$M_t = \Delta W \Delta \sigma_b A, \tag{35}$$

where

$$\Delta \sigma_b = \sigma_p - \sigma_d \tag{36}$$

is the effective shear stress, and A is the area of the total ruptured plane of the fault.

The far-field radiation from the beginning of slip to final slip D for the ruptured portion of the fault of area ΔA is proportional to the time rate of change of seismic moment

$$\Delta \dot{M}_0 = \mu \Delta \dot{u} \Delta A. \tag{37}$$

If we also integrate $\Delta \dot{M}_0$ over the entire time interval of rupture and the entire rupture surface, we obtain the usual representation for scalar seismic moment

$$M_0 = \mu D A, \tag{38}$$

where M_0 is the scalar seismic moment due to a dislocation source of final slip D.

The dimensionless ratio k of the torque moment rate in the radiation from the decrease of stress in the breakdown process with an effective shear stress change of $\Delta \sigma_b$, thickness of breakdown zone of ΔW to the usual seismic moment rate from the same dislocation source with rigidity μ, is

$$k = \frac{\Delta \dot{M}_t}{\Delta \dot{M}_0}. \tag{39}$$

To estimate the torque moment rate and seismic moment rate, we find from equations (33) and (37)

$$\Delta \dot{M}_t \approx \frac{\Delta W \Delta \sigma_b \Delta A}{T_s'}, \qquad \Delta \dot{M}_0 \approx \frac{\mu D \Delta A}{T_s},$$

where $T_s' = t_s' - t_p$ is the characteristic time for stress change (i.e., time for completing the breakdown), and $T_s = t_s - t_p$ is the usual rise time (i.e., the time for the completion of slip at a point on the fault). We estimate T_s and T_s' roughly by $T_s \approx D/v_f$, $T_s' \approx D_c/v_f$, where v_f is the advancing velocity of the crack tip (i.e., the rupture velocity). Thus,

$$k = \frac{\Delta W \Delta \sigma_b}{\mu D_c}, \tag{40}$$

where we have used $T_s/T_s' \approx D/D_c$ by virtue of $T_s \approx D/v_f$ and $T_s' \approx D_c/v_f$.

The effective shear stress $\Delta \sigma_b$ has several estimates. According to an early estimate by Kanamori (1994), $\Delta \sigma_b \approx$ 2 to 20 MPa. The estimate of Ohnaka (2003) is $\Delta \sigma_b \approx 1$ to 100 MPa. Recently, Rice *et al.* (2005) gave $\Delta \sigma_b \approx$ 100 MPa. In our numerical estimate, we adopt

- $D_c \approx 0.5$ m (Mikumo and Yagi, 2003; Fukuyama and Mikumo, 2007).
- $\Delta W \approx 200$ m (Li and Leary, 1990; Li *et al.*, 1990; Li and Vidale, 1996; Li *et al.*, 1997).
- $\Delta \sigma_b \approx 60$ MPa (Kanamori, 1994; Ohnaka, 2003; Rice *et al.*, 2005).
- $\mu \approx 3 \times 10^4$ MPa.

Substitution of these values into equation (40) yields $k \approx 4/5$. Field investigations from some great earthquakes show that the width of the fault zone or the thickness of the strength-weakening zone ΔW ranges from several hundred meters to several kilometers. In view of these comments the k value, at least for some larger earthquakes, may be even larger than the present estimate.

The total moment from the torque moment M_t and seismic moment M_0 for the entire rupture process and the entire ruptured area is equivalent to a dislocation source with seismic moment

$$M_0' = \frac{1}{2} M_t + M_0, \tag{41}$$

where the factor of $1/2$ is introduced because the radiation from a single couple with unit moment is half the radiation of a double couple with the same amount of seismic moment for each pair of couples.

If the contribution to the total moment from the torque moment is not taken into account, the seismic moment due to a dislocation source is estimated by equation (38). Thus, the ratio of seismic moment estimated from far-field radiation, taking into account the contribution from the torque moment to that simply from the dislocation source, is

$$\frac{M_0'}{M_0} = 1 + \frac{M_t}{2M_0} \approx 1 + \frac{k}{2} \cdot \frac{D_c}{D}. \tag{42}$$

The ratios M_0'/M_0 are listed in Table 1 for some representative values of the final slip D for the case $k = 0.8$. The overestimate of the total moment magnitude is only about $(2/3)\lg(M_0'/M_0) = (2/3)\lg(1.2) \approx 0.06$ in the most optimistic case of importance of the torque moment. The influence is not pronounced on a logarithmic scale.

The results obtained here have two implications. The first is that in usual waveform analysis, the use of the dislocation model alone would overestimate seismic moment and consequently the final slip D if the contribution to the far-field radiation from the torque moment is not taken into account. The overestimate may be as much as a factor of 1.2 to

Table 1
Ratios of M_0'/M_0

D (m)	D/D_c	M_0'/M_0
1	2	1.20
2	4	1.10
3	6	1.07
4	8	1.05
5	10	1.04

1.04 as D ranges from 1 to 5 m. These results may explain the discrepancies between seismic moments or final slips estimated from usual waveform analysis using the dislocation model alone and field observations or geodetic measurements. The second is that in usual waveform analysis, the use of the dislocation model alone would introduce an extra seismic moment rate and consequently an extra slip rate of as much as a factor of $k/2 \approx 0.4$ of the usual seismic moment rate and the usual slip rate during the time interval for completion of the breakdown process if the contribution to the far-field radiation from the torque moment is not taken into account. This will in turn influence the calculation of seismic energy radiated from earthquake events.

Discussion and Conclusions

We have reexamined the two canons of the seismological literature that elastic displacements in the far-field are proportional to slip velocities on the dynamical fault surface, and that dynamical in-plane slip on an earthquake fault has a double-couple body force equivalent. Taking into account the fact that if faulting occurs on a fault of finite thickness and if a strength-weakening zone exists near the advancing crack tip, we have shown that in addition to the usual double-couple term, there is a single-couple term in the body force equivalence in the far-field displacement, which is proportional to the time rate of increase of stress drop. We have shown that the single-couple equivalent does not violate principles of Newtonian mechanics because the torque imbalance in the single couple is counterbalanced by rotations within the fault zone. The crack therefore radiates torque waves.

We have estimated the ratio of the torque moment rate radiated during the breakdown process to the usual seismic moment rate from the same rupturing fault and the ratio of seismic moment released with contribution from the torque moment released to that simply from the dislocation source. These results imply that if the contribution to the far-field radiation from the torque moment is not taken into account in usual waveform analysis, the use of the dislocation model alone would overestimate seismic moment and consequentially the final slip. It would introduce an extra seismic moment rate and consequentially an extra slip rate. This will in turn affect calculations of seismic energy radiated from earthquake events. We have also shown that frictional torques accumulated in a fault zone of finite width during an interearthquake interval are relaxed through the development of torque or rotation waves radiated as shear waves during the time-dependent, frictional, or stress-weakening (relaxation) part of the fracture process near the tips of advancing cracks. Torque waves are small during the more familiar frictional sliding interval, where the dynamical friction remains relatively constant.

The relaxation of torques within the fault may play an important role in driving the rotation of material in the fault zone and dramatically changing the dynamic friction in the fault zone, and the radiation of torque waves from an advancing strength-weakening zone before the occurrence of a large earthquake may give a clue to account for rotational phenomena, which have been reported in some historical documents (Galitzin, 1912, p. 75; Bullen, 1953, pp. 135, 251; Richter, 1958, p. 213; Bouchon and Aki, 1982; Takeo and Ito, 1997; Takeo, 1998; Teisseyre *et al.*, 2003; Igel *et al.*, 2007).

Data and Resources

All data used in this article came from published sources listed in the references.

Acknowledgments

Yun-Tai Chen was supported by the National Natural Science Foundation of China (No. 40774021).

References

Aki, K. (1966). Generation and propagation of *G* waves from Niigata earthquake of June 16, 1964. 2. Estimation of earthquake movement, released energy, and stress-strain drop from *G* wave spectrum, Tokyo University, *Bull. Earthq. Res. Inst.* **44,** 23–88.

Aki, K., and P. Richards (1980). *Quantative Seismology Theory Methods*, Vols. **1** and **2,** W. H. Freeman, San Francisco, 932 pp.

Born, M., and E. Wolf (1959). *Principles of Optics*, Pergamon Press, London, 803 pp.

Bouchon, M., and K. Aki (1982). Strain, tilt, and rotation associated with strong ground motion in the vicinity of earthquake faults, *Bull. Seismol. Soc. Am.* **72,** 1717–1738.

Bullen, K. E. (1953). *An Introduction to the Theory of Seismology*, Second Ed., Cambridge University Press, New York, 296 pp.

Burridge, R., and L. Knopoff (1964). Body force equivalents for seismic dislocations, *Bull. Seismol. Soc. Am.* **51,** 69–84.

Cochard, A., and R. Madariaga (1996). Complexity of seismicity due to highly rate-dependent friction, *J. Geophys. Res.* **101,** no. B11, 25,321–25,366.

Cochard, A., H. Igel, B. Schuberth, W. Suryanto, A. Velikoseltsev, U. Schreiber, I. Wassermann, F. Scherbaum, and D. Vollmer (2006). Rotational motions in seismology: Theory, observation, simulation, in *Earthquake Source Asymmetry, Structural Media and Rotation Effects*, R. Teisseyre, M. Takeo, and E. Majewski (Editors), Springer-Verlag, Berlin, Heidelberg, New York, The Netherlands, 582 pp.

Day, S. M. (1982). Three-dimensional simulation of spontaneous rupture: the effect of nonuniform prestress, *Bull. Seismol. Soc. Am.* **72,** 1881–1902.

de Hoop, A. T. (1958). *Representation Theorems for the Displacement in An Elastic Solid and Their Application to Elastodynamic Diffraction Theory*, *Doctoral Thesis*, Technische Hogeschool, Delft, The Netherlands, 84 pp.

Fukuyama, E., and T. Mikumo (2007). Slip-weakening distance estimated at near-fault stations, *Geophys. Res. Lett.* **34,** L09302, doi 10.1029/2006GL029203.

Galitzin, B. B. (1912). Lecture on seismometry, in *Selected Works of B. B. Galitzin*, Vol. **2,** 1–228, Academy of Sciences, USSR, Moscow, 487 pp. (in Russian).

Haskell, N. A. (1964). Total energy and energy spectral density of elastic wave radiation from propagating faults, Part I, *Bull. Seismol. Soc. Am.* **54,** 1811–1841.

Haskell, N. A. (1966). Total energy and energy spectral density of elastic wave radiation from propagating faults, Part II, A statistical source model, *Bull. Seismol. Soc. Am.* **56,** 125–140.

Heaton, T. (1990). Evidence for and implication of self-healing pulses of slip in earthquake rupture, *Phys. Earth Planet. Interi.* **64,** 1–20.

Igel, H., A. Cochard, J. Wassermann, A. Flaws, U. Schreiber, A. Velikoseltsev, and N. Pham Dinh (2007). Broad-band observations of earthquake-induced rotational ground motions, *Geophys. J. Int.* **168,** 182–196.

Kanamori, H. (1994). Mechanics of earthquakes, *Ann. Rev. Earth Planet Sci.* **22,** 207–237.

Knopoff, L. (1956). Diffraction of elastic waves, *J. Acous. Soc. Am.* **28,** 217–229.

Knopoff, L., and F. Gilbert (1960). First motions from seismic sources, *Bull. Seismol. Soc. Am.* **50,** 117–134.

Kostrov, B. V. (1970). The theory of the focus for tectonic earthquakes, *Izv. Phys. Solid Earth* 258–267, (in Russian).

Kostrov, B. V. (1974). Seismic moment and energy of earthquake and seismic flow of rock, *Izv. Phys. Solid Earth*, 13–21, (in Russian).

Li, Y.-G., and P. C. Leary (1990). Fault zone trapped seismic waves, *Bull. Seismol. Soc. Am.* **80,** 1245–1271.

Li, Y.-G., and J. E. Vidale (1996). Low-velocity fault-zone guided waves: numerical investigations of trapping efficiency, *Bull. Seismol. Soc. Am.* **86,** 371–378.

Li, Y.-G., W. L. Ellsworth, C. H. Thurber, P. E. Malin, and K. Aki (1997). Fault-zone guided waves from explosions in the San Andreas fault at Parkfield and Cienega valley, California, *Bull. Seismol. Soc. Am.* **87,** 210–222.

Li, Y.-G., P. C. Leary, K. Aki, and P. E. Malin (1990). Seismic trapped modes in the Oroville and San Andreas fault zones, *Science* **249,** 763–766.

Love, A. E. H. (1927). *A Treatise on the Mathematical Theory of Elasticity*, 4th ed., Cambridge University Press, New York, 643 pp.

Maruyama, T. (1963). On the force equivalents of dynamical elastic dislocations with reference to the earthquake mechanism, Tokyo University *Bull. Earthq. Res. Inst.* **41,** 46–86.

Mikumo, T., and T. Miyatake (1978). Dynamic rupture process on a three-dimensional fault with non-uniform frictions and near-field seismic waves, *Geophys. J. R. Astr. Soc.* **54,** 417–458.

Mikumo, T., and Y. Yagi (2003). Slip-weakening distance in dynamic rupture of in-slab normal-faulting earthquakes, *Geophys. J. Int.* **155,** 443–455.

Nowacki, W. (1986). *Theory of Asymmetric Elasticity*, Pergamon Press, Oxford, 384 pp.

Ohnaka, M. (2003). A constitutive scaling law and a unified comprehension for frictional slip failure, shear fracture of intact rock, and earthquake rupture, *J. Geophys. Res.* **108,** no. B2, 2080, doi 10.1029/2000JB000123.

Ohnaka, M., and T. Yamashita (1989). A cohesive zone model for dynamic shear faulting based on experimentally inferred constitutive relation and strong motion source parameters, *J. Geophys. Res.* **94,** 4089–4104.

Ohnaka, M., H. Akatsu, A. Mochizuki, F. Tagashira, and Y. Yamamoto (1997). A constitutive law for the shear failure of rock under lithospheric condition, *Tectonophysics* **277,** 1–27.

Rice, J. R., C. G. Sammis, and R. Parsons (2005). Off-fault secondary failure induced by a dynamic slip-pulse, *Bull. Seismol. Soc. Am.* **95,** 109–134, doi 10.1785/0120030166.

Richter, C. F. (1958). *Elementary Seismology*, W. H. Freeman, San Francisco, 768 pp.

Stauder, W., and G. A. Bollinger (1964). The *S*-wave project for focal mechanism studies, earthquakes of 1962, *Bull. Seismol. Soc. Am.* **54,** 2198–2208.

Stauder, W., and G. A. Bollinger (1966). The *S*-wave project for focal mechanism studies, earthquakes of 1963, *Bull. Seismol. Soc. Am.* **56,** 1363–1371.

Stokes, G. G. (1849). On the dynamical theory of diffraction, *Trans. Camb. Phil. Soc.* **9,** 1–62, Reprinted in *Stokes' Mathematical and Physical Papers, 2*(1883). Cambridge, 243–328.

Stratton, J. A. (1941). *Electromagnetic Theory*, McGraw-Hill, New York, 615 pp.

Takeo, M. (1998). Ground rotational motions recorded in near-source region of earthquake, *Geophys. Res. Lett.* **25,** 789–792.

Takeo, M., and H. M. Ito (1997). What can be learned from rotational motions excited by earthquakes? *Geophys. J. Int.* **129,** 319–329.

Teisseyre, R., J. Suchcicki, K. P. Teisseyre, J. Wiszniowski, and P. Palangio (2003). Seismic rotation waves: Basic elements of theory and recording, *Ann. Geophys.* **46,** 671–685.

Wald, D. J., and T. H. Heaton (1994). Spatial and temporal distribution of slip for the 1992 Landers, California earthquake, *Bull. Seismol. Soc. Am.* **84,** 668–691.

Venkataraman, A., and H. Kanamori (2004). Observational constraints on the fracture energy of subduction zone earthquakes, *J. Geophys. Res.* **109,** B05302, doi 10.1029/2003JB002549.

Yamashita, T. (1976). On the dynamic process of fault motion in the presence of friction and inhomogeneous initial stress. Part I. Rupture propagation, *J. Phys. Earth* **24,** 417–444.

Zheng, G., and J. R. Rice (1998). Conditions under which velocity weakening friction allows a self-healing versus a cracklike mode of rupture, *Bull. Seismol. Soc. Am.* **88,** no. 6, 1466–1483.

Institute of Geophysics and Planetary Physics
University of California
Los Angeles, California 90095-1567
lknopoff@igpp.ucla.edu
(L.K.)

Institute of Geophysics
China Earthquake Administration
5 Minzudaxue Nan Road, Haidian District
Beijing 100081, China
chenyt@cea-igp.ac.cn
(Y.-T.C.)

Manuscript received 28 September 2008